

OPEN
ACCESS

Eco-friendly Removal of Methylene Blue Using Alginate-Activated Natural Clay Composite

Rasidah^{a*}, Jumiat^a, Wahyu Nugroho^a, Retno Agnestisia^a, Karelius^a, Roki Alfanaar^a, Rendy Muhamad Iqbal^a

Abstract. Methylene blue is a poisonous, persistent, and non-biodegradable dye frequently found in textile industry wastewater that significantly influences the emergence of various environmental and health problems. Therefore, precautions must be taken to reduce the amount of methylene blue in the wastewater. Compositing clay into alginate produces an eco-friendly adsorbent, alginate-activated clay composite beads (Ag-AC 1-5%), successfully removing methylene blue. XRD and FTIR spectroscopy characterization results show that illite, a family of 2:1 clay minerals, is a primary constituent of activated clay. However, FTIR spectroscopy shows that alginate has mannuronic acid residue characteristics. Several batch experiments were carried out to evaluate the effect of the alginate: clay ratio and pH solution on the percentage of methylene blue removal. The higher the proportion of activated clay on the composite, the better the adsorption of methylene blue. The alginate-activated clay composite beads eliminate methylene blue up to 99.03% at the optimum pH=5, showing a potential alternative methylene blue adsorbent with a wide range of adsorption pH compared to the original material alone.

Keywords : Alginate-clay composite, eco-friendly adsorbent, methylene blue adsorption, methylene blue removal

^aChemistry Department, Universitas Palangka Raya, Palangka Raya 73112, Central Kalimantan, Indonesia

Correspondence and requests for materials should be addressed to Rasidah (email: rasidah@mipa.upr.ac.id).

Introduction

Water pollution is primarily caused by industrial liquid waste. Even though the textile sector does not produce much solid waste, it contributes to the vast volumes of liquid waste that pollute waterways and cause several environmental issues. Together with numerous other industrial pollutants, textile dyes are extremely harmful, may cause cancer, and also contribute to environmental deterioration and a host of illnesses in both humans and animals [1], [2], [3]. Dyes are also harmful to the health of aquatic animals. For example, *Catla catla* develops micro-nuclei and undergoes histological alterations when exposed to dyes [4]. According to reports, dyes can produce highly toxic aromatic compounds with mutagenic and carcinogenic qualities when combined with synthetic intermediates and the byproducts of their breakdown [5]. Therefore, industrial liquid waste, especially dyes from the textile industry, must be treated before being discharged into the environment.

Methylene blue, a cationic dye often found in textile industry wastewater, is a toxic organic compound with stable and non-biodegradable properties [6]. In the coloring process, only 25% of this compound is used, while the remaining 75% will be discharged into the water as waste. According to regulatory norms and recommendations established by the majority of nations and organizations such as WHO, UNEP, EPA-USA, CPCB-India, NWQMS-Australia, and MOE-Japan, the acceptable threshold value for the concentration of methylene blue dye in water is less than 1 mg/L or equivalent to 1 mg/kg. At concentrations exceeding 5 mg/kg, the monoamine oxidase-inhibiting properties of methylene blue dye can cause deadly serotonin poisoning in humans [6]. However, MAO inhibitors may cause severe serotonin poisoning or serotonin syndrome if administered intravenously at a dosage greater than the advised concentration [7]. The prolonged exposure to concentrated methylene blue solutions in human reproduction has been reported to harm the ability of sperm to migrate more efficiently [8]. Regarding the environment, dye molecules may reduce photosynthesis by obstructing sunlight from penetrating the water's surface. Then, the entire ecosystem collapsed due to the detrimental effects on the production and survival of phytoplankton, which is the basis of the food chain.

Therefore, if the use of methylene blue as a dye in the textile industry is not balanced with the management of the waste produced, it will emerge with various environmental and health problems, so handling efforts are needed to minimize the amount of waste.

Methylene blue has a very high solubility in water, so it is difficult to remove using conventional methods [6], [9]. Various methods have been developed to reduce or even eliminate methylene blue dye in aqueous solutions, including adsorption [10], [11], [12], ultrafiltration [13], [14], [15], degradation [16], [17], [18], coagulation [19], [20], [21], and photocatalysis methods [22], [23], [24]. Chemical removal techniques, both photochemical and non-photochemical, can produce secondary pollutants, according to an evaluation of elimination techniques from 240 reviews and/or research-published articles [6]. On the other hand, the sensitivity of enzymes to pH is a characteristic of biological approaches. Adsorption is widely used and developed since it is one of the most successful and regarded as the most effective in terms of ease of preparation and low operating costs compared to other methods developed [25]. The adsorption method is the most excellent option for processing methylene blue waste since it is also more straightforward to use and degradable.

The selection of the type of adsorbent is seen from the perspective of effectiveness and selectivity in adsorption and is expected to be cheap and easy in the manufacturing process [26], [27], [28], [29]. Adsorbents often found in nature, such as clay, are economically feasible to use as adsorbent materials. Apart from its abundant availability, clay also has many advantages, namely high cation exchange capacity, large surface area, and chemical and mechanical stability [30]. These advantages make clay widely used as an adsorbent for the adsorption of dyes such as methylene blue.

Clay is typically employed in powdered form to improve its surface area and adsorption capacity. The applicability of clay in powder form is limited, though, as it is challenging to separate from the liquid phase following the adsorption process. Therefore, new methods must be developed to facilitate the separation process while preserving or improving its efficacy. Another way to get around clay's drawbacks is to encapsulate clay powder in sodium alginate to transform it into a methylene blue, polymer-based form. Alginate is also well-known as a supportive substance frequently utilized in environ-

mental and biological applications. In addition to simplifying the separation process, alginate provides several benefits when added to clay, including simple formulation, mild gelation conditions, non-toxicity, affordability, and the ability to function as an adsorbent [31], [32], [33], [34], [35]. Alginate has active sites in the form of hydroxyl and carboxyl groups, which can be used to bind and adsorb metal ion contaminants and dyes [36], [37], [38]. So, compositing clay with alginate is expected to provide a more efficient, stable, and eco-friendly method to remove methylene blue from solutions than using clay or alginate alone.

Experimental

Synthesis and characterization of clay-alginate composite beads. A certain amount of activated clay (AC) that has been synthesized following the procedure of the previous study [39] is mixed into an alginate solution of 1% to obtain clay concentrations of 0, 1, 2, 3, 4, and 5% (w/v), respectively, and stirred for 2 hours. The dispersed mixture was then dropwise into 200 mL of 0.1 M CaCl₂ solution using a 4 mm diameter syringe. Then, the beads were washed with aquadest and left for 30 minutes in 0.1 M CaCl₂ solution. Alginate beads (Alg) and alginate-clay composite beads (Alg-AC) 1, 2, 3, 4, and 5% were washed with 0.7% NaCl solution and characterized using FTIR and XRD instruments.

Determination of optimum adsorption pH. A total of 0.03 grams of samples of Ag, AC, and Alg-AC (1, 2, 3, 4, and 5%) were put into each 10 mL of methylene blue (MB) 60 ppm, whose acidity had been adjusted to pH 1, 3, 5, 7, and 9. Then, the mixture was shaken for 3 hours at room temperature. Next, the absorbance of the filtrate was measured using a UV-Vis Spectrophotometer to calculate the % adsorption removal of

MB.

Result and Discussion

Synthesis of clay-alginate composite beads.

The results of the synthesis of alginate beads without (Alg) and with the addition of activated clay (Alg-AC) are shown in Figure 1. Physically, it can be seen that Alg beads have a transparent, clear colour appearance with a chewy texture typical of alginate, which is rich in mannuronic acid monomers. In contrast, Alg-AC is cream-coloured with a stiffer texture (less chewy) than Alg beads. The clay used to synthesize Alg-AC adsorbents in this study has a yellow colour characteristic. The clay is activated physically and chemically to dissolve impurities or compounds that can cover the clay pores, so it is expected to improve the characteristics and adsorption capacity of the clay.

The sharp peaks in Figure 2 indicate that the crystallinity of the activated clay is very good. At first glance, the diffraction pattern shown is similar to that obtained from the activation of natural clay from North Maurisu Village, NTT [40], and yellow clay from Central Kalimantan [41]. However, from the characterization results of the XRD diffraction peaks of activated clay in this study, the highest peaks of activated natural clay minerals were obtained at angles $2\theta = 20.88, 26.68, \text{ and } 50.16$, corresponding to the characteristics of illite minerals. The peaks showed higher intensity than the reference due to the presence of the smallest amount of quartz, which has similar or overlapping diffraction patterns, so the total intensity observed is the sum of the intensities from illite and quartz.

According to [42], the distinctive clay mineralogies and their chemical and physical properties are controlled by how Si-O tetrahedra and Al-O octahedra stack together. For this reason, clay minerals are often described by the ratio of Si:Al layers in their structure, and illite is one of the most common

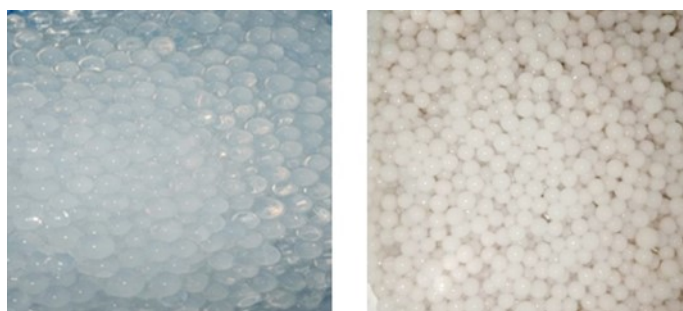


Figure 1. Alginate and clay-alginate composite beads

and highly abundant mineral types of Si:O with a ratio of 2:1 clay minerals. Then, the peak-overlapping issues, especially at $2\theta = 20,88$; $26,68$; and $50,16$ between illite and quartz diffraction peaks, can be overcome by using Rietveld refinement with standard crystallographic models to determine the intensity of individual illite accurately [43]. Thus, it can be understood that illite is the main component of activated clay minerals in this study, and quartz is a minor mineral whose presence is found together with clay because both minerals are often formed in the same geological environment.

One of the challenges in using clay as an adsorbent is its fragile structure or tendency to clump. Alginate helps stabilize clay by forming a gel network that increases the mechanical strength and functionality of the material. Alginate is a polysaccharide composed of mannuronic acid and guluronic acid monomers (Figure 3) with three types of groupings, namely alternating mannuronic and guluronic residue groups (MGMGM...), guluronic acid (GGGGG...) and mannuronic acid (MMMM...) [44], [45], [46]. The monomers of mannuronic acid (M) and guluronic acid (G) are composed in different proportions depending on the type of seaweed used as raw material, age, and location where the seaweed grows [45]. Young tissues are rich in M blocks, and the percentage of G blocks increases with the tissue's age. In addition, the M/G ratio and the concentration of divalent cations in alginate gels significantly affect cross-linking density, mechanical properties, and pore size. Alginate rich in M blocks will form a softer and more elastic gel than that rich in G blocks, resulting in a hard and brittle gel [47]. The higher the M/G ratio, the smaller the average pore size [48]. Then, the longer the chain, the greater the molecular weight and the greater the viscosity value [49]. In other words, the arrangement and proportion of two different chemical structures of mannuronic acid and guluronic acid units will give alginate unique properties. The next subchapter will discuss in more detail the characteristics of alginate monomers in this study.

The effect of adding clay on the characteristics of the functional groups of clay-alginate composite beads Activated natural clay, alginate (without clay), and alginate clay composite beads, namely Alg-AC 1, 2, 3, 4, and 5%, were characterized using a Fourier Transform Infrared

(FTIR) instrument to identify functional groups and types of vibrations contained in the tested samples. FTIR spectra of activated clay (AC), alginate (Alg), and clay-alginate composite beads (Alg-AC) 1, 2, 3, 4, and 5% can be seen in Figure 4. Based on these absorption peaks, the alginate contains mannuronic acid residues, while the examined activated clay belongs to the 2:1 clay mineral family, namely illite, a mica-like clay mineral.

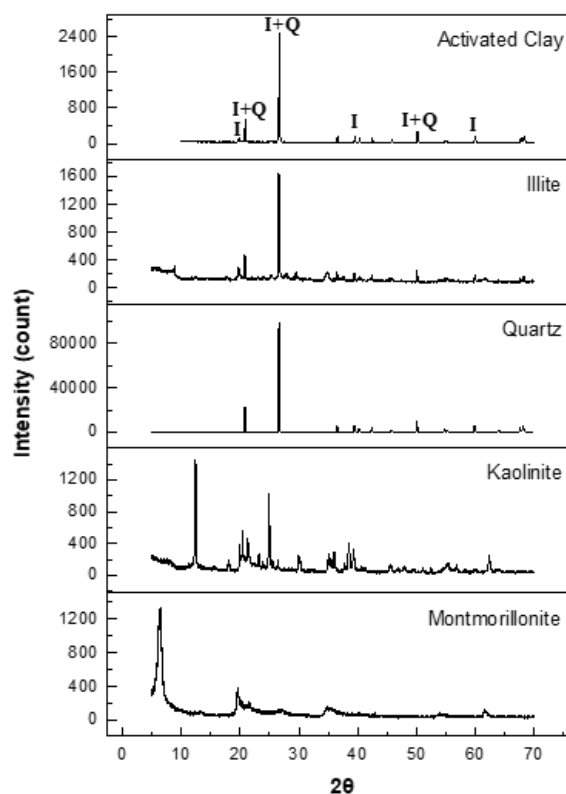


Figure 2. XRD patterns of the sample (activated clay) and material references

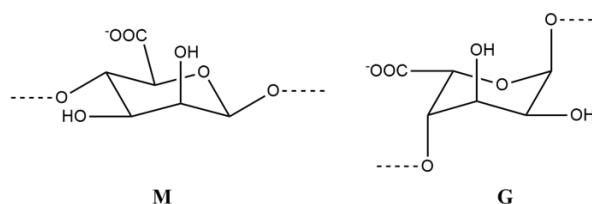


Figure 3. The monomers of alginate [50]

Alginate contains many free hydroxyl (-OH) and carboxyl (-COOH) groups, which enable it to form intramolecular hydrogen bonds [51]. A broad absorption peak in the 3343 cm^{-1} is a stretching vibration in the hydroxyl group (O-H). Meanwhile, asymmetrical and symmetrical stretching vibrations of the COO^- group cause absorption at wavenumbers 1594 and 1420 cm^{-1} . Furthermore, the absorption at wavenumber 1077 cm^{-1} is a stretch-

ing vibration of the C-O-C group originating from the pyranose ring in the structure of mannuronic and guluronic acids in alginate. The presence of absorption around 1023 cm^{-1} is caused by stretching vibrations in glycosidic bonds, while the absorption at wavenumber 817 cm^{-1} shows a relationship to mannuronic acid residues identified in the wavenumber range of $800\text{ to }820\text{ cm}^{-1}$ ((Huang et al., 2017; Leal et al., 2008; Mollah et al., 2023). Thus, the alginate used is a type of alginate that has a structure with mannuronic acid residues that have smaller pore sizes or larger adsorption surface areas in proportion to the higher M/G ratio.

The peaks of bands at 3694 , 3625 , 2369 , 1634 , 1031 , 916 , and 777 cm^{-1} indicated that illite was present as the main component of clay. These similar clear sign results were reported by previous researchers [55], [56]. The type of 2:1 of layer clays such as illite will show broad absorption in $2600 \sim 3650\text{ cm}^{-1}$ accompanied by a shoulder peak; meanwhile, the 1:1 of layer clays (i.e., kaolinite) always display a narrow and weak absorption in 3600 cm^{-1} . Most importantly, according to the FTIR absorption peak graph, a peak of 916 cm^{-1} appeared only in samples containing more than 6% illite [55].

The significant band strength around 3343 , 1594 , and 1420 cm^{-1} in Figure 4 indicated the presence of alginate. Meanwhile, the availability bands around 916 , 777 , 693 , 526 , and 455

cm^{-1} are characteristic of clay, suggesting that alginate has already been composited with clay. The absorption shift in the region around $3300 - 3360\text{ cm}^{-1}$ in the Alg-AC 1-5% spectra is related to the difference in the environment of -OH bound to the Al-octahedral atoms on the silicate surface or inter-layer. Furthermore, the characteristic peaks of quartz at wavenumbers around 1085 and 462 cm^{-1} [57] or higher, around 1097 and 469 cm^{-1} [58], cannot be observed clearly. It is likely due to the quartz absorption overlapping with the strong absorption of illite at wavenumber around 1033 and 455 cm^{-1} .

The strong absorption in the $950\text{-}250\text{ cm}^{-1}$ region is the stretching vibration of M-O (where M = Si or Al and other metals), which involves the main motion of the oxygen atom Si-O [59]. In this case, the emergence of an absorption peak at wavenumber $914\text{-}916\text{ cm}^{-1}$ is the Al-OH bending vibration. Absorption at this number indicates the occurrence of the arrangement of the clay framework structure due to the release of water molecules due to calcination and acid activation [60]. Indirectly, it shows the increasingly homogeneous environment of silica-alumina minerals due to the reduction of minerals and impurities due to the calcination and acid activation processes. Then, the absorption at wavenumber 777 cm^{-1} shows the presence of stretching vibrations of O-Si-O, which is characteristic of microcrystalline SiO_2 , $690\text{-}692\text{ cm}^{-1}$ are stretching vibrations of Si-O and the bands at $519\text{-}528$ and $439\text{-}451\text{ cm}^{-1}$ are due to Al-O-Si and Si-O-Si bending vibrations indicate that the activated

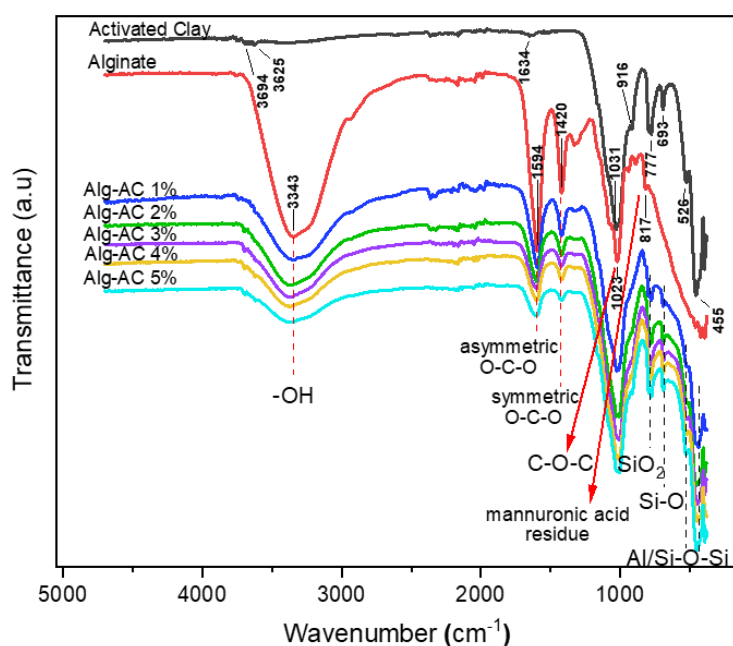


Figure 4. FTIR spectra of activated natural clay, alginate, and alginate-clay composite beads (Ag-AC 1-5%)

clay has been successfully incorporated into alginate.

The effect of adding clay on the optimum pH conditions for adsorption of alginate-composite beads. In this research, pH variations were carried out at 1, 3, 5, 7, and 9 to determine the optimum pH conditions required by the adsorbent to adsorb MB. During the adsorption process, the concentration of MB slowly decreases, which can be seen from the reduction in the intensity of the blue colour in the solution (Figure 5). The adsorption effectiveness of MB by Alg (alginate without clay), AC (activated clay), and Alg-AC 1, 2, 3, 4, and 5% (clay-alginate compo-

site) beads across varying pH levels can be seen in Figure 6. These results also indirectly illustrate the charge characteristic on the surface of alginate, activated clay, and alginate-activated clay composite at the specified pH variations.

Figures 5 and 6 show that alginate has a lower adsorption capacity than activated clay and a better MB removal percentage with a wider pH range after being composited with activated clay. The adsorption of MB by alginate at low pH (pH=1) increases with increasing pH until it reaches an optimum uptake of 66.49% at pH 7 and then decreases at a higher pH (pH 9). Meanwhile, adsorption of MB by activated clay at low pH (pH=1) showed a % re-

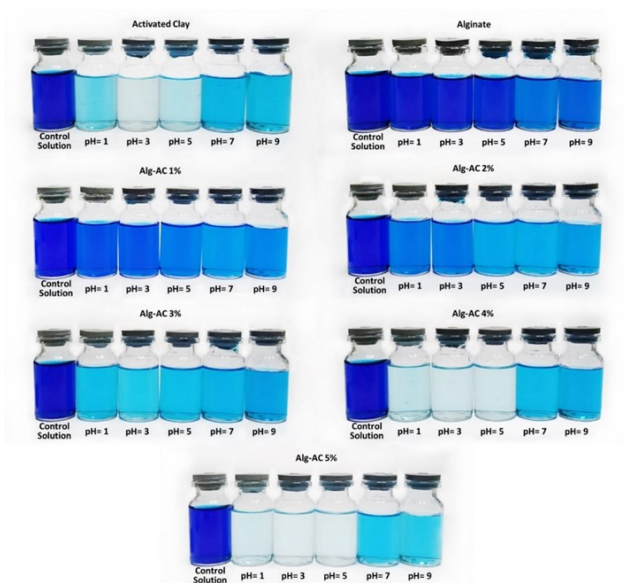


Figure 5. The visual appearance of MB removal using activated natural clay, alginate, and alginate-clay composite beads (Alg-AC 1-5%) at various pH conditions.

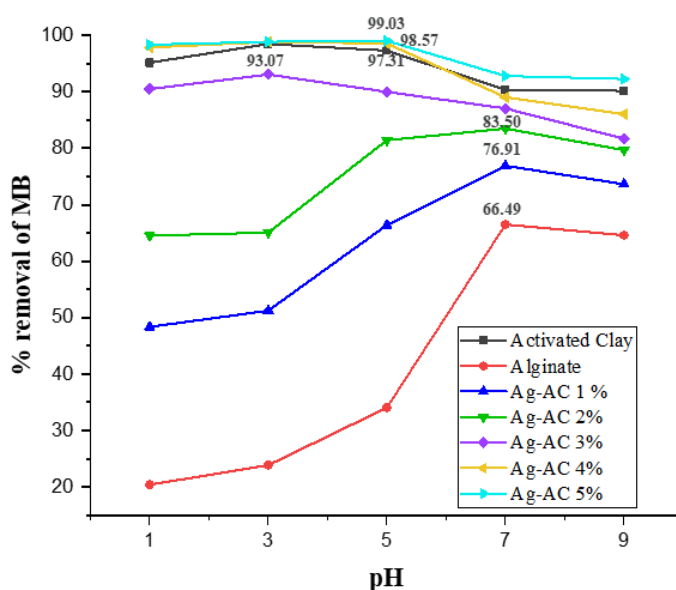


Figure 6. Percentage of MB removal at various pH variations by (a) alginate; (b) Alg-AC 1%; (c) Alg-AC 2%; (d) Alg-AC 3%; (e) Alg-AC 4%; (f) activated clay (AC); (g) Alg-AC 5% beads

removal more than 4x higher than alginate. It was relatively constant as the pH increased, with the optimum pH for adsorption at pH 5, 97.31%. After this pH, adsorption continues to decrease to 90.17% at pH=9. The Alg-AC 3% adsorbent also demonstrated similar adsorption efficiency and was very clear in the Alg-AC 4% and Alg-AC 5% adsorbents. Figure 6 shows that the % MB removal of Alg-AC 4% and Alg-AC 5% is much higher than activated clay at optimum pH (pH=5). It is also confirmed that the adsorption of MB by Alg-AC 4% and Alg-AC 5% is more affected by activated clay than alginate. It is also assumed that increasing the clay percentage even higher will not significantly increase adsorption efficiency.

The adsorption data (Figure 6) demonstrated a correlation between the % removal of MB and the pH value. The acidity (pH) level is an important parameter controlling adsorption. The value of the level of acidity (pH) can influence changes in the charge distribution on the surface of the adsorbent and MB, which is caused by the occurrence of deprotonation and protonation reactions in functional groups. At Alg-AC 1% and Alg-AC 2%, the optimum pH for MB adsorption occurs at pH=7, similar to Alg. In contrast, when adding a higher concentration of clay (above 2%), the optimum pH for adsorption occurs at a more acidic (pH=5), resembling the optimum pH for MB adsorption by AC. It can be explained by looking at the pH where the surface charge is zero or point of zero charge (pzc) values of alginate and clay. The pzc value for Ca-alginate, illite, and quartz is 6.5 [61], 2.5 [62], and varied around <4.5 [63], respectively. These mean that alginate will have a negative charge to attract positive charges of MB at pH=7, illite at pH=3, and quartz will occur at pH=5. As a result, the optimum pH adsorption of Alg, Alg-AC 1%, and Alg-AC 2% towards MB occurs at pH=7, whereas AC at pH=3 and Alg-AC 3-5% at pH=5.

The undissociated MB molecules are more prevalent at pH=1 (99%) and pH=3 (86%), according to the speciation diagram and molecular structure of the MB [64]. It is consistent with alginate's smaller adsorption toward MB at certain pH values. Electrostatic repulsion between the cationic dye molecules and the adsorbent surface causes a decrease in dye adsorption when the adsorbent surface is positively charged [65]. On the contrary, MB was highly adsorbed by clay even though the surface charge was positive,

indicating that MB was possibly adsorbed by other mechanisms than electrostatic attraction. Then, compared to the percentage of MB removed at pH=1 and pH=3, the cationic species of MB is more prevalent at pH=5 (92%), and it can be assumed that electrostatic attraction also plays a role in the more excellent result in the percentage of MB removed by AC clay. Meanwhile, the cationic species of MB is the only species that exists at pH > 5 and is highly attracted to the negative charge of alginate at pH=7, indicating that MB adsorption of alginate follows an electrostatic attraction mechanism. At the higher pH, the negative charge of the clay and alginate saturated with MB, and the desorption occurred while MB was being adsorbed.

CONCLUSION

The adsorption capacity of alginate-activated clay composite beads (Alg-AC) increases towards methylene blue compared to the original material before the composite. The higher the percentage of activated clay in the composite, the better the percentage of removal of methylene blue. The composition of Alg-AC 5% had the highest percentage of removal MB of 99.03% at pH = 5. Raising the clay composition above 5% may not significantly increase the amount of elimination MB and the optimum pH range of adsorption (pH=1-5).

Acknowledgements

The authors are grateful for the laboratory support from Chemistry Laboratory, Universitas Palangka Raya.

Author Contributions

All the authors have contributed sufficiently to this research, from coming up with the idea, collecting the data, supervising, and producing the paper.

References

- [1] B. Lellis, C. Z. Fávoro-Polonio, J. A. Pamphile, and J. C. Polonio, "Effects of textile dyes on health and the environment and bioremediation potential of living organisms," *Biotechnology Research and Innovation*, vol. 3, no. 2, pp. 275–290, Jul. 2019, doi: 10.1016/j.biori.2019.09.001.
- [2] S. Khan and A. Malik, "Toxicity evaluation of

textile effluents and role of native soil bacterium in biodegradation of a textile dye," *Environmental Science and Pollution Research*, vol. 25, no. 5, pp. 4446–4458, Feb. 2018, doi: 10.1007/s11356-017-0783-7.

[3] R. Kishor et al., "Ecotoxicological and health concerns of persistent coloring pollutants of textile industry wastewater and treatment approaches for environmental safety," *J Environ Chem Eng*, vol. 9, no. 2, Apr. 2021, doi: 10.1016/j.jece.2020.105012.

[4] B. Jagruti, "Evaluation of azo dye toxicity using some haematological and histopathological alterations in *Catla catla*," *International Journal of Biological, Food, Veterinary and Agricultural Engineering*, vol. 9, no. 5, 2015.

[5] T. Ito, Y. Adachi, Y. Yamanashi, and Y. Shimada, "Long-term natural remediation process in textile dye-polluted river sediment driven by bacterial community changes," *Water Res*, vol. 100, pp. 458–465, 2016, doi: 10.1016/j.watres.2016.05.050.

[6] P. O. Oladoye, T. O. Ajiboye, E. O. Omotola, and O. J. Oyewola, "Methylene blue dye: Toxicity and potential elimination technology from wastewater," *Results in Engineering*, vol. 16, Dec. 2022, doi: 10.1016/j.rineng.2022.100678.

[7] A. M. McDonnell, I. Rybak, M. Wadleigh, and D. C. Fisher, "Suspected serotonin syndrome in a patient being treated with methylene blue for ifosfamide encephalopathy," *Journal of Oncology Pharmacy Practice*, vol. 18, no. 4, pp. 436–439, Dec. 2012, doi: 10.1177/1078155211433231.

[8] Y. R. Sheynkin, C. Starr, P. S. Li, and M. Goldstein, "Effect of methylene blue, indigo carmine, and renografin on human sperm motility," *Urology*, vol. 53, pp. 214–217, 1999, doi: [https://doi.org/10.1016/S0090-4295\(98\)00414-2](https://doi.org/10.1016/S0090-4295(98)00414-2).

[9] M. M. Hassan and C. M. Carr, "A critical review on recent advancements of the removal of reactive dyes from dyehouse effluent by ion-exchange adsorbents," Oct. 01, 2018, Elsevier Ltd. doi: 10.1016/j.chemosphere.2018.06.043.

[10] E. Altıntig, H. Altundag, M. Tuzen, and A. Sari, "Effective removal of methylene blue from aqueous solutions using magnetic loaded activated carbon as novel adsorbent," *Chemical Engi-*

neering Research and Design, vol. 122, pp. 151–163, 2017, doi: 10.1016/j.cherd.2017.03.035.

[11] P. K. Jaseela, J. Garvasis, and A. Joseph, "Selective adsorption of methylene blue (MB) dye from aqueous mixture of MB and methyl orange (MO) using mesoporous titania (TiO₂) – poly vinyl alcohol (PVA) nanocomposite," *J Mol Liq*, vol. 286, 2019, doi: 10.1016/j.molliq.2019.110908.

[12] X. Wan, Z. Rong, K. Zhu, and Y. Wu, "Chitosan-based dual network composite hydrogel for efficient adsorption of methylene blue dye," *Int J Biol Macromol*, vol. 222, pp. 725–735, 2022, doi: <https://doi.org/10.1016/j.ijbiomac.2022.09.213>.

[13] S. M. Doke and G. D. Yadav, "Novelties of combustion synthesized titania ultrafiltration membrane in efficient removal of methylene blue dye from aqueous effluent," *Chemosphere*, vol. 117, no. 1, pp. 760–765, 2014, doi: 10.1016/j.chemosphere.2014.10.029.

[14] E. Oyarce, B. Butter, P. Santander, and J. Sánchez, "Polyelectrolytes applied to remove methylene blue and methyl orange dyes from water via polymer-enhanced ultrafiltration," *J Environ Chem Eng*, vol. 9, no. 6, Dec. 2021, doi: 10.1016/j.jece.2021.106297.

[15] S. Parakala, S. Moulik, and S. Sridhar, "Effective separation of methylene blue dye from aqueous solutions by integration of micellar enhanced ultrafiltration with vacuum membrane distillation," *Chemical Engineering Journal*, vol. 375, Nov. 2019, doi: 10.1016/j.cej.2019.122015.

[16] R. Kishor et al., "Efficient degradation and detoxification of methylene blue dye by a newly isolated ligninolytic enzyme producing bacterium *Bacillus albus* MW407057," *Colloids Surf B Biointerfaces*, vol. 206, Oct. 2021, doi: 10.1016/j.colsurfb.2021.111947.

[17] A. Samide, B. Tutunaru, C. Tigae, R. Efrem, A. Moanță, and M. Drăgoi, "Removal of methylene blue and methyl blue from wastewater by electrochemical degradation," *Environment Protection Engineering*, vol. 40, no. 4, Mar. 2020, doi: 10.37190/epe140408.

[18] A. S. Van Der Maas, N. J. R. Da Silva, A. S. V. Da Costa, A. R. Barros, and C. A. Bomfeti, "The degradation of methylene blue dye by the strain of *Pleurotus* sp. with potential application in bioremediation processes," *Revista Ambiente Agua*, vol. 13, pp. 1–10, 2018, doi: 10.4136/1980-993X.

- [19] S. Ihaddaden, D. Aberkane, A. Boukerroui, and D. Robert, "Removal of methylene blue (basic dye) by coagulation-flocculation with biomaterials (bentonite and *Opuntia ficus indica*)," *Journal of Water Process Engineering*, vol. 49, p. 102952, 2022, doi: <https://doi.org/10.1016/j.jwpe.2022.102952>.
- [20] N. Jorge, A. R. Teixeira, L. Marchão, P. B. Tavares, M. S. Lucas, and J. A. Peres, "Removal of methylene blue from aqueous solution by application of plant-based coagulants," *Engineering Proceedings*, vol. 19, no. 1, 2022, doi: [10.3390/ECP2022-12659](https://doi.org/10.3390/ECP2022-12659).
- [21] M. Alizadeh, E. Ghahramani, M. Zarrabi, and S. Hashemi, "Efficient de-colorization of methylene blue by electro-coagulation method: comparison of iron and aluminum electrode," *Iran. J. Chem. Chem. Eng.* Alizadeh M. et al, vol. 34, no. 1, 2015, doi: <https://doi.org/10.30492/ijcce.2015.12679>.
- [22] M. A. E. Wafi, M. A. Ahmed, H. S. Abdel-Samad, and H. A. A. Medien, "Exceptional removal of methylene blue and p-aminophenol dye over novel TiO₂/RGO nanocomposites by tandem adsorption-photocatalytic processes," *Mater Sci Energy Technol*, vol. 5, pp. 217–231, Jan. 2022, doi: [10.1016/j.mset.2022.02.003](https://doi.org/10.1016/j.mset.2022.02.003).
- [23] O. A. Yildirim and E. Pehlivan, "Removal of methylene blue using a novel generation photocatalyst based on nano-SnO₂/wild plumb kernel shell biochar composite," *J Dispers Sci Technol*, vol. 44, no. 14, pp. 2748–2759, 2023, doi: [10.1080/01932691.2022.2144878](https://doi.org/10.1080/01932691.2022.2144878).
- [24] J. Ramírez-Aparicio, J. E. Samaniego-Benítez, M. A. Murillo-Tovar, J. L. Benítez-Benítez, E. Muñoz-Sandoval, and M. L. García-Betancourt, "Removal and surface photocatalytic degradation of methylene blue on carbon nanostructures," *Diam Relat Mater*, vol. 119, p. 108544, 2021, doi: <https://doi.org/10.1016/j.diamond.2021.108544>.
- [25] G. Mckay, J. F. Porter, and G. R. Prasad, "The removal of dye colours from aqueous solutions by adsorption on low-cost materials," *Water Air Soil Pollut*, vol. 114, pp. 423–438, 1999.
- [26] S. Wang, J. Dou, T. Zhang, S. Li, and X. Chen, "Selective Adsorption of Methyl Orange and Methylene Blue by Porous Carbon Material Prepared From Potassium Citrate," *ACS Omega*, vol. 8, no. 38, pp. 35024–35033, Sep. 2023, doi: [10.1021/acsomega.3c04124](https://doi.org/10.1021/acsomega.3c04124).
- [27] G. Mosoarca, C. Vancea, S. Popa, M. Gheju, and S. Boran, "Syringa vulgaris leaves powder a novel low-cost adsorbent for methylene blue removal: isotherms, kinetics, thermodynamic and optimization by Taguchi method," *Sci Rep*, vol. 10, 2020, doi: [10.1038/s41598-020-74819-x](https://doi.org/10.1038/s41598-020-74819-x).
- [28] C. P. Sagita, L. Nulandaya, and Y. S. Kurniawan, "Efficient and low-cost removal of methylene blue using activated natural kaolinite material," *Journal of Multidisciplinary Applied Natural Science*, vol. 1, no. 2, pp. 69–77, Jul. 2021, doi: [10.47352/jmans.v1i2.80](https://doi.org/10.47352/jmans.v1i2.80).
- [29] P. Sharma, H. Laddha, M. Agarwal, and R. Gupta, "Selective and effective adsorption of malachite green and methylene blue on a non-toxic, biodegradable, and reusable fenugreek galactomannan gum coupled MnO₂ mesoporous hydrogel," *Microporous and Mesoporous Materials*, vol. 338, p. 111982, 2022, doi: <https://doi.org/10.1016/j.micromeso.2022.111982>.
- [30] S. Barakan and V. Aghazadeh, "The advantages of clay mineral modification methods for enhancing adsorption efficiency in wastewater treatment: a review," Jan. 01, 2021, Springer Science and Business Media Deutschland GmbH. doi: [10.1007/s11356-020-10985-9](https://doi.org/10.1007/s11356-020-10985-9).
- [31] S. Vahidhabanu, D. Karuppasamy, A. I. Adeogun, and B. R. Babu, "Impregnation of zinc oxide modified clay over alginate beads: A novel material for the effective removal of congo red from wastewater," *RSC Adv*, vol. 7, no. 10, pp. 5669–5678, 2017, doi: [10.1039/c6ra26273b](https://doi.org/10.1039/c6ra26273b).
- [32] N. Yang et al., "The fabrication of calcium alginate beads as a green sorbent for selective recovery of Cu(II) from metal mixtures," *Crystals (Basel)*, vol. 9, no. 5, May 2019, doi: [10.3390/cryst9050255](https://doi.org/10.3390/cryst9050255).
- [33] R. da Silva Fernandes, M. R. de Moura, G. M. Glenn, and F. A. Aouada, "Thermal, microstructural, and spectroscopic analysis of Ca²⁺ alginate/clay nanocomposite hydrogel beads," *J Mol Liq*, vol. 265, pp. 327–336, Sep. 2018, doi: [10.1016/j.molliq.2018.06.005](https://doi.org/10.1016/j.molliq.2018.06.005).
- [34] H. Han, M. K. Rafiq, T. Zhou, R. Xu, O. Mašek, and X. Li, "A critical review of clay-based composites with enhanced adsorption performance for metal and organic pollutants," *J Hazard Mater*, vol. 369, pp. 780–796, May 2019, doi: [10.1016/j.jhazmat.2019.05.005](https://doi.org/10.1016/j.jhazmat.2019.05.005).

j.jhazmat.2019.02.003.

[35] I. T. K. Ge, M. W. Nugraha, N. Ahmad Kamal, and N. S. Sambudi, "Composite of kaolin/sodium alginate (SA) beads for methylene blue adsorption," *ASEAN Journal of Chemical Engineering*, vol. 19, no. 2, pp. 100–109, 2019, doi: 10.22146/ajche.51457.

[36] A. A. Elzatahry, E. A. Soliman, M. S. M. Eldin, and M. E. Youssef, "Experimental and simulation study on removal of methylene blue dye by alginate micro-beads," *Journal of American Science*, vol. 6, no. 10, pp. 845–851, 2010, [Online]. Available: <https://www.researchgate.net/publication/259891705>

[37] X. Gao, C. Guo, J. Hao, Z. Zhao, H. Long, and M. Li, "Adsorption of heavy metal ions by sodium alginate based adsorbent—a review and new perspectives," *Int J Biol Macromol*, vol. 164, pp. 4423–4434, 2020, doi: 10.1016/j.ijbiomac.2020.09.046.

[38] S. Asadi, S. Eris, and S. Azizian, "Alginate-Based Hydrogel Beads as a Biocompatible and Efficient Adsorbent for Dye Removal from Aqueous Solutions," *ACS Omega*, vol. 3, no. 11, pp. 15140–15148, Nov. 2018, doi: 10.1021/acsomega.8b02498.

[39] I. M. Sadiana, A. H. Fatah, and K. Karelius, "Sintesis Komposit Lempung Alam Magnetit sebagai Adsorben.... (I Made Sadiana, dkk," *Sains dan Terapan Kimia*, vol. 11, pp. 90–102, 2017, doi: <http://dx.doi.org/10.20527/jstk.v11i2.4042>.

[40] M. M. Kolo, M. S. Batu, and M. M. Taus, "Karakterisasi Mineral Lempung Desa Maurisu Utara, Kabupaten Timor Tengah Utara Teraktivasi KOH sebagai Bahan Baku Adsorben," *Jurnal Cystal: Publikasi Penelitian Kimia dan Terapannya*, vol. 5, no. 1, pp. 14–21, 2023.

[41] K. Karelius, "Extraction and characterization natural clay of central kalimantan as one of alternatives additives of geopolimer concrete," *Jurnal Pendidikan Teknologi dan Kejuruan BALANGA*, vol. 5, pp. 1–10, 2017.

[42] J. Wimpenny, "Clay minerals," in *Encyclopedia of Earth Sciences Series*, Springer Science and Business Media B.V., 2016, pp. 1–11. doi: 10.1007/978-3-319-39193-9_51-1.

[43] B. Patarachao et al., "XRD analysis of illite-smectite interstratification in clays from oil

sands ores," *Advances in X-Ray Analysis*, no. 62, pp. 22–31, 2019, [Online]. Available: www.dxcicdd.com

[44] G. O. Phillips and P. A. Williams, *Handbook of Hydrocolloids*. in Woodhead Publishing Series in Food Science, Technology and Nutrition. Woodhead Publishing, 2009. [Online]. Available: <https://books.google.co.id/books?id=3k-kAgAAQBAJ>

[45] K. I. Draget, O. Smidsrød, and G. Skjåk-Brñk, "Polysaccharides and polyamides in the food industry: properties, production, and patents," A. Steinbüchel and S. K. Rhee, Eds., Weinheim: Wiley-VCH, 2005, ch. Alginates from Algae.

[46] H. Grasdalen, B. Larsen, and O. Smidsrød, "13C-N.M.R. Studies of monomeric composition and sequence in alginate," *Carbohydr Res*, vol. 89, pp. 179–191, 1981, doi: [https://doi.org/10.1016/S0008-6215\(00\)85243-X](https://doi.org/10.1016/S0008-6215(00)85243-X).

[47] F. A. Johnson, D. Q. M. Craig, and A. D. Mercer, "Characterization of the block structure and molecular weight of sodium alginates," *Journal of Pharmacy and Pharmacology*, vol. 49, no. 7, pp. 639–643, 1997, doi: 10.1111/j.2042-7158.1997.tb06085.x.

[48] M. D. Torres, S. Kraan, and H. Dominguez, *Sustainable Seaweed Technologies: Cultivation, Bio-refinery, and Applications*, 1st ed. Elsevier, 2020. doi: 10.1016/C2018-0-01462-0.

[49] D. J. McHugh, *Production and utilization of products from commercial seaweeds*, 1st ed. Food and Agriculture Organization of the United Nations, 1987.

[50] N. A. Ibrahim, A. A. Nada, and B. M. Eid, "Polysaccharide-Based Polymer Gels and Their Potential Applications," 2018, ch. 4, pp. 97–126. doi: 10.1007/978-981-10-6083-0_4.

[51] E. D. T. Atkins, I. A. Nieduszynski, W. Mackie, K. D. Parker, and E. E. Smolko, "Structural Components of Alginic Acid. I. The Crystalline Structure of Poly-p-D-Mannuronic Acid. Results of X-Ray Diffraction and Polarized Infrared Studies," *Biopolymers*, vol. 12, pp. 1865–1878, 1973.

[52] H. Huang, I. U. Grün, M. Eilersieck, and A. D. Clarke, "Measurement of total sodium alginate in restructured fish products using Fourier Transform Infrared Spectroscopy," *EC Nutr*, vol. 11, pp. 33–45, 2017.

[53] D. Leal, B. Matsuhira, M. Rossi, and F. Caruso, "FT-IR Spectra of Alginic Acid Block Fractions in Three Species of Brown Seaweeds," *Carbohydr Res*,

vol. 343, no. 2, pp. 308–316, Feb. 2008, doi: 10.1016/j.carres.2007.10.016.

[54] M. Z. I. Mollah, M. R. I. Faruque, D. A. Bradley, M. U. Khandaker, and S. Al Assaf, "FTIR and Rheology Study of Alginate Samples: Effect of Radiation," *Radiation Physics and Chemistry*, vol. 202, Jan. 2023, doi: 10.1016/j.radphyschem.2022.110500.

[55] G. Jozanikohan and M. N. Abarghooei, "The Fourier transform infrared spectroscopy (FTIR) analysis for the clay mineralogy studies in a clastic reservoir," *J Pet Explor Prod Technol*, vol. 12, no. 8, pp. 2093–2106, Aug. 2022, doi: 10.1007/s13202-021-01449-y.

[56] M. Pineau et al., "Estimating kaolinite crystallinity using near-infrared spectroscopy," in *51st Lunar and Planetary Science Conference*, 2020. [Online]. Available: <https://www.researchgate.net/publication/339712567>

[57] J. Ojima, "Determining of crystalline silica in respirable dust samples by Infrared Spectrophotometry in the presence of interferences," *J Occup Health*, vol. 45, no. 2, pp. 94–103, Mar. 2003, doi: 10.1539/joh.45.94.

[58] G. A. P. K. Wardhani, N. Nurlela, and M. Azizah, "Silica content and structure from corn-cob ash with various acid treatment (HCl, HBr, and citric acid)," *Molekul*, vol. 12, no. 2, pp. 174–181, Nov. 2017, doi: 10.20884/1.jm.2017.12.2.382.

[59] E. Eren, B. Afsin, and Y. Onal, "Removal of lead ions by acid activated and manganese oxide-coated bentonite," *J Hazard Mater*, vol. 161, no. 2–3, pp. 677–685, Jan. 2009, doi: 10.1016/j.jhazmat.2008.04.020.

[60] N. J. Saikia et al., "Characterization, beneficiation and utilization of a kaolinite clay from Assam, India," *Appl Clay Sci*, vol. 24, no. 1–2, pp. 93–103, 2003, doi: 10.1016/S0169-1317(03)00151-0.

[61] A. Zyoud et al., "Photocatalytic degradation of aqueous methylene blue using ca-alginate supported ZnO nanoparticles: point of zero charge role in adsorption and photodegradation," *Environmental Science and Pollution Research*, vol. 30, no. 26, pp. 68435–68449, Jun. 2023, doi: 10.1007/s11356-023-27318-1.

[62] S. A. Hussain, D. Sahinde, and G.

Ozbayoglu, "Zeta Potential Measurements on Three Clays from Turkey and effects of clays on coal flotation," *J Colloid Interface Sci*, vol. 184, pp. 535–541, 1996, doi: <https://doi.org/10.1006/jcis.1996.0649>.

[63] M. Kosmulski, "pH-dependent surface charging and points of zero charge. III. Update," *J Colloid Interface Sci*, vol. 298, no. 2, pp. 730–741, Jun. 2006, doi: 10.1016/j.jcis.2006.01.003.

[64] J. J. Salazar-Rabago, R. Leyva-Ramos, J. Rivera-Utrilla, R. Ocampo-Perez, and F. J. Cerino-Cordova, "Biosorption mechanism of Methylene Blue from aqueous solution onto White Pine (*Pinus durangensis*) sawdust: Effect of operating conditions," *Sustainable Environment Research*, vol. 27, no. 1, pp. 32–40, Jan. 2017, doi: 10.1016/j.serj.2016.11.009.

[65] Ü. Geçgel, G. Özcan, and G. Ç. Gürpnar, "Removal of methylene blue from aqueous solution by activated carbon prepared from pea shells (*Pisum sativum*)," *J Chem*, 2013, doi: 10.1155/2013/614083.